LUND UNIVERSITY

Acute Myocardial Infarction: The Relationship between Duration of Ischaemia and Infarct Size in Humans - Assessment by MRI and SPECT

Hedström, Erik

2005

[Link to publication](#)

Citation for published version (APA):
Hedström, E. (2005). *Acute Myocardial Infarction: The Relationship between Duration of Ischaemia and Infarct Size in Humans - Assessment by MRI and SPECT*. Department of Clinical Physiology, Lund University.

Total number of authors:
1

Acute Myocardial Infarction

The Relationship between Duration of Ischaemia and Infarct Size in Humans – Assessment by MRI and SPECT

ERIK HEDSTRÖM

LUND UNIVERSITY

Doctoral Thesis
2005

Department of Clinical Physiology
Lund University, Sweden

Faculty opponent
Dr Andrew E. Arai, National Institutes of Health, Bethesda, MD, USA

The public defense of this thesis for the degree Doctor of Philosophy in Medicine will, with due permission from the Faculty of Medicine at Lund University, take place in Föreläsningssal 1, Lund University Hospital, on Saturday, 1 October 2005, at 09.00.

Cover:
SPECT polar plots indicating myocardium at risk (black) in the otherwise well perfused myocardium (yellow). Final infarct size from DE-MRI is shown in white, where brightness indicates transmurality. The longer the duration of ischaemia, the larger the final infarct size. Please see page 26 for details.

We cling to our own point of view,
as though everything depended on it.
Yet our opinions have no permanence;
like autumn and winter,
they gradually pass away.

—Chuang Tzu

Contents

List of Publications

This thesis is based on the following papers, which in the text will be referred to by their Roman numerals.

My contribution to the studies was to take part in designing the studies, perform the inclusion of the acutely reperfused and clinical patient populations, take part in the experimental work, perform the MR imaging, analyse all data, and write the manuscripts.

I. E. Hedstrom, J. Palmer, M. Ugander, H. Arheden. Myocardial SPECT perfusion defect size compared to infarct size by delayed gadolinium-enhanced magnetic resonance imaging in patients with acute or chronic infarction. *Clin Physiol Funct Imaging.* 2004;24:380-386.

II. E. Hedstrom, K. Astrom-Olsson, H. Ohlin, F. Frogner, M. Carlsson, T. Billgren, S. Jovinge, P. Cain, G.S. Wagner, H. Arheden. Identification of peak biochemical markers in acutely reperfused patients provides accurate estimation of myocardial infarct size as determined by delayed contrast-enhanced magnetic resonance imaging. *Submitted.*

III. E. Hedstrom, H. Arheden, R. Eriksson, L. Johansson, H. Ahlstrom, T. Bjerner. The importance of perfusion in myocardial viability studies using delayed contrast-enhanced magnetic resonance imaging. *Submitted.*

IV. E. Hedstrom, F. Frogner, H. Ohlin, K. Astrom-Olsson, H. Arheden. *In-vivo* demonstration of the relationship between duration of ischemia and myocardial infarct size in humans. *Manuscript.*

Summary

The effect of duration of ischaemia on final infarct size is well established in animal studies, but not fully evaluated in humans. Delayed contrast-enhanced magnetic resonance imaging (DE-MRI) can be used to distinguish between viable and non-viable myocardium and thus to quantify infarct size. We therefore used DE-MRI to investigate how duration of ischaemia affects final infarct size normalized to myocardium at risk in humans (Paper IV). The results showed that 20–40 % of myocardium at risk was infarcted after 2–3 hours of occlusion, indicating that a major part of myocardium at risk may be salvaged if reperfusion is performed within the first few hours of occlusion.

In order to study infarct evolution in humans, we first investigated the correlation between perfusion defect size assessed by myocardial single photon emission computed tomography (SPECT) perfusion imaging with final infarct size by DE-MRI (Paper I), showing that measurements by the two methods do not differ much for revascularized myocardial infarction.

Biochemical markers of cardiac injury are used to estimate myocardial infarct size. The agreement between cumulative as well as peak values of biochemical markers and DE-MRI in patients with an occluded coronary artery was studied for Paper II. We showed that in order to estimate infarct size, serial measurements may be substituted by acquisitions at 3, 6, and 12 hours after reperfusion, saving both cost and time in the clinical setting.

Finally, experimental infarction in pig was studied in collaboration with Uppsala University in order to provide a basis for further investigations on how MR contrast agents distribute in perfused and non-perfused myocardium in humans (Paper III). This study showed that perfusion is needed for delivery of contrast agent, and that the non-perfused myocardium, despite absence of contrast agent in this region, appears bright when nulling the signal from viable perfused myocardium using inversion-recovery DE-MRI.

Populärvetenskaplig sammanfattning

En hjärtinfarkt, dvs död hjärtmuskel, uppstår då en del av hjärtats muskel inte blodförsörjs, exempelvis genom att en propp bildats i ett av hjärtats blodkärl. Detta tillstånd bör behandlas snarast möjligt för att rädda största möjliga del av hjärtmuskeln, eftersom en större infarkt innebär sämre pumpfunktion vilket ger patienten sämre prognos. Tidsförloppet för en hjärtinfarkts utveckling hos människa har inte klargjorts tidigare. Vi har nu visat att 20–40 % av det område som hotas att bli infarkt, blir det efter 2–3 timmar. Det är alltså av största vikt att behandla patienten inom de första timmarna efter det att proppen uppstått (studie IV).

För att möjliggöra studium av infarktutveckling hos människa behövde vi säkerställa korrelationen mellan två olika metoder, nämligen SPECT (avbildning av hjärtmuskelns genomblödning med hjälp av radioaktiv isotop) och infarktmätning med magnetisk resonanstomografi (MR). Vi visade i studie I att mätningar med dessa två metoder ger jämförbara resultat.

Vid en hjärtinfarkt släpps skademarkörer ut i blodet och dessa mäts för att uppskatta hur stor infarkt som har uppkommit. För att säkerställa uppskattningen av infarktstorleken bör serieprover tas med täta intervall. Vi visade i studie II att man för patienter som behandlats med ballongvidgning kan ersätta serieprover med enstaka prover utan att det påverkar bedömningen av infarktstorlek. Detta kan ge besparingar i både tid och pengar.

För att studera hur de kontrastmedel som används vid infarktdiagnostik med MR fungerar, genomfördes i samarbete med Uppsala Universitet studie III. Denna studie visade att inget kontrastmedel kommer in i ett område som saknar blodförsörjning, något som tidigare inte varit helt klarlagt. Detta område kan dessutom misstolkas som infarkt. Fortsatta studier inom området är av värde för att öka förståelsen kring hur kontrastmedelförstärkt MR fungerar.

Abbreviations

ACE	angiotensin-converting enzyme
CKMB	creatine kinase isoenzyme MB_{mass}
CT	computed tomography
cTnT	cardiac troponin T
DE-MRI	delayed contrast-enhanced magnetic resonance imaging
DOTA	1,4,7,10-tetraazacyclododecane-1,4,7,10-tetraacetic acid
DTPA	diethylenetriaminepentaacetic acid
DTPA-BMA	{bis-[2-(carboxymethylmethylcarbamoyl methylamino)ethyl]amino}acetic acid
ECG	electrocardiography
FBP	filtered backprojection
GPIIb/IIIa	glycoprotein IIb/IIIa
GRE	gradient-recalled echo
IR	inversion recovery
LV	left ventricle
LVWV	left ventricular wall volume
MRI	magnetic resonance imaging
PCI	percutaneous coronary intervention
PET	positron emission tomography
R_1	longitudinal magnetization relaxation rate
ΔR_1	$R_{1,time} - R_{1,baseline}$
RF	radio frequency
SD	standard deviation
SI	signal intensity
SPECT	single photon emission computed tomography
TI	inversion time
TIMI	Thrombolysis in Myocardial Infarction
TTC	triphenyltetrazolium chloride

Chapter 1

Introduction

1.1   Ischaemic heart disease

Reimer et al.[84] showed in 1977 that a myocardial infarct evolves gradually over time with a "wave front" from the endocardium toward the epicardium. Final infarct size is therefore related not only to the size of the region subjected to ischaemia, i.e. the myocardium at risk, but also to the time from onset of occlusion to restoration of perfusion to the ischaemic myocardium.

   The expression "time is muscle" is therefore relevant, and the concept of the "golden hour", during which a very large portion of myocardium at risk may be salvaged, is well known for several species,[6,34,43,48,55,67,83–85,94] but less studied in humans. The studies GISSI-1[1] and ISIS-2[2] showed that fibrinolytic therapy within 1 hour from onset of symptoms results in more than 50 % reduction of mortality. Results from previous studies indicate that treatment within 6 hours from onset of symptoms give a mortality reduction twice that of treatment 6–12 hours after onset of pain.[16] Overall, this shows that also in humans, early reperfusion is of great value. The more quantitative relationship between duration of ischaemia and final infarct size in humans is, however, not fully evaluated.

Pathophysiology

The most common cause of myocardial infarction is rupture of an atherosclerotic plaque with formation of a thrombus leading to occlusion of a coronary artery.[111] The rupture of a plaque results in exposure of collagen, lipids, smooth muscle cells, and tissue factor to the blood, leading to activation of platelets and the coagulation system.[23,36,82] Glycoprotein (GP) IIb/IIIa receptors on the surface of the platelets enable aggregation of platelets through cross-bridges of fibrinogen, and

several vasoactive and pro-coagulative mediators are released. Treatment resulting in inhibition of these receptors is therefore of interest.

The occlusion of a coronary artery results in insufficient blood supply in relation to the demand of the contracting myocytes. Ischaemia occurs, and if blood flow is not restored fast enough, the result is myocardial cell necrosis. The dead myocytes are replaced by connective tissue over time and loss of wall motion occurs. If the infarct is large enough, heart failure may ensue.

Except for duration of ischaemia, other factors such as the site of occlusion and collateral supply contribute to final infarct size. The site of occlusion is of importance for the size of the myocardium at risk. A more gradual development of occlusive atherosclerotic disease may, however, permit recruitment of collateral vessels, which in turn may provide perfusion to myocardium otherwise at risk during occlusion of a coronary artery.[81] Collateral flow may therefore decrease the final infarct size. Different species have different amounts of collateral supply[67] and may therefore show diverse results when the impact of duration of ischaemia on final infarct size is assessed.

Diagnosis

The diagnosis of myocardial infarct may be performed by several methods. Electrocardiography (ECG) is a widely available method that is easy to use. Its sensitivity and specificity may be increased with various scoring systems, even though its original diagnostic performance is reasonably good. Biochemical markers of cardiac injury are easily acquired and have high sensitivity and specificity, especially the troponins. The biochemical markers used today are preferably creatine kinase isoenzyme MB_{mass} (CKMB), cardiac troponin T (cTnT) or cardiac troponin I.[4] CKMB is a cytosolic protein that is released when the membrane of the myocyte ruptures, and cTnT exists both as a cytosolic protein and bound to the tropomyosin complex. Therefore cTnT is elevated for a longer time than CKMB. The time-to-peak and release into peripheral blood over time are influenced by the grade of reperfusion.[49] For sizing of myocardial infarct, it is therefore of importance to acquire the "true" peak value, which may be accomplished by serial blood sampling.

By using single photon emission computed tomography (SPECT),[39,68] the perfusion defect may be visualized, both as myocardium at risk in the acute setting, and later for estimation of infarct size. Echocardiography[93] can be used to evaluate wall motion, but is highly user dependent. The method is however widely available and mobile equipment is used, facilitating the examination. Positron emission tomography (PET)[8] is mainly a research tool, but increasingly used in the clinical setting for absolute quantification of perfusion. Using computed tomography (CT), perfusion and coronary arteries may be visualized. The CT has

high negative predictive value and is therefore useful to rule out coronary artery disease.[90] Coronary angiography can be used for visualizing the coronary arteries and show stenosis or occlusion. However, discrepancies between grade of stenosis and perfusion exist.[3] The advantage of invasive angiography is that it is possible to intervene during the examination. By magnetic resonance imaging (MRI), perfusion, function, infarct size, as well as other parameters, may be quantified. One important advantage compared with invasive angiography, SPECT, CT, and PET, is that no ionizing radiation is used for imaging.

Therapy

The aim of the therapy is to restore perfusion and to reduce myocardial oxygen demand. Even though blood flow is spontaneously restored in some patients through activation of the fibrinolytic system, medical or mechanical reperfusion is of great value for saving myocardium at risk. The drawback of pharmacological reperfusion is that the earlier drugs needed infusion and thereby precious time passed. The newer drugs are given as bolus doses, and time is no longer a major issue, even though it is not possible to directly assess whether epicardial blood flow is fully restored. By percutaneous coronary intervention (PCI), however, this is possible. During fluoroscopy, a balloon is inflated at the location of the occlusion whereby the artery is dilated. Thereafter, a stent (a wire net) is expanded into the vessel wall to prevent reoccurrence of occlusion. During this procedure, a GPIIb/IIIa inhibitor may be administered, leading to decreased aggregation of platelets and thereby increased success of reperfusion, also at the endocardial level.[73] If the GPIIb/IIIa inhibitor is administered before hospital admission, it is possible to acheive restoration of epicardial flow even before PCI, and thereby a larger amount of myocardium at risk may be salvaged.

Myocardial infarct mortality has been reduced throughout the years by introducing specialized coronary care units, and drugs such as thrombocyte aggregation inhibitors, angiotensin-converting enzyme (ACE) inhibitors, beta receptor inhibitors, and statins.

1.2 Single photon emission computed tomography

There are several different ways to handle the acquisition and quantification of SPECT images.[27] In this short review, however, only the properties of the system used in the present studies are mentioned.

The SPECT is a method used to diagnose coronary artery disease. Compared with planar imaging, the diagnostic value is increased by extracting the plane of interest from the surrounding structures.[17,95] Background contribution is reduced

and quantification of perfusion and function is greatly improved. The sensitivity and specificity, as well as positive and negative predictive values, are all very high.[78,107]

^{99m}Tc-tetrofosmin

Several radiopharmaceuticals may be used for SPECT perfusion imaging, the more common being ^{201}Tl, and ^{99m}Tc bound either to sestamibi or tetrofosmin.[9,103] The ideal marker of perfusion should be distributed in the myocardium proportionally to blood flow, have a high grade of extraction from blood and be retained in the myocardium over a time period sufficient for imaging, have a rapid elimination to make a repeat examination possible, and give a low whole-body radiation dose.

The ^{99m}Tc-tetrofosmin used in the present studies distribute in the myocardium in proportion to blood flow[98] and is taken up by the viable myocytes, most possibly by a potential-driven transport of the lipophilic cation[109] and binding to the mitochondria.

The isotope is retained in the myocardium for at least 4 hours and imaging is therefore possible during this time span.[102] The effective $T_{1/2}$ *in vivo* is 2.4 hours. Very little change in myocardial distribution is seen over time.[104]

Imaging and quantification of perfusion defect size

For acquisition of images, the technique relies on the gamma ray emissions from the radiopharmaceutical, and their interaction with the detector. The images are acquired by rotation of the detectors, set at 90° angle, in a circular fashion around the supine patient. The detectors acquire planar images during a certain time, and then moves to the next predefined position along its orbital path. When a photon is absorbed in one of the crystals of the detector, scintillation occurs and the energy and spatial location is recorded.[101] By changing from ^{201}Tl to ^{99m}Tc with an energy of 140 keV an improved spatial resolution has been obtained.

The sampling is gated to ECG, which results in 8 frames per cardiac cycle (temporal resolution approximately 125 ms) and thereby gives information about cardiac function. Traditionally, reconstruction to transverse images is performed by filtered backprojection (FBP) using a Fourier transform with a ramp filter and a low-pass filter (e.g. Butterworth filter). The ramp filter is inherent to the reconstruction algorithm, whereas the low-pass filter removes noise from the image. We used an iterative method for image reconstruction – Maximum-Likelihood Expectation-Maximization, initialized with FBP – applied for increased image quality.[69,106]

The image consists of a 64×64 matrix with a digital pixel resolution of approximately 5 mm. It should be noted that SPECT has limitations in both spatial and temporal resolution compared with MRI. Also, partial volume effects may occur since the pixel value is an integrated value of the measured activity.[46]

The quantification of perfusion defect size can be performed by using Auto-Quant (ADAC, Milpitas, CA, USA) or other available automatic methods. Myocardium at risk during occlusion of a coronary artery, can be measured by SPECT. The isotope is administered during occlusion and since the myocardial uptake is fast and redistribution minimal, as mentioned above, the image acquired also after opening of the occlusion represents the perfusion of the myocardium during occlusion.[97]

1.3   Magnetic resonance imaging

Magnetic resonance imaging is based on a quantum mechanical process, but its macroscopic manifestation is under most circumstances well described by classical physics. Herein, a basic understanding is presented, and more details can be found in the literature.[10,41,87]

Magnetic resonance imaging originates from the discovery that nuclei with an uneven mass number and an uneven charge number possess a spin, and thereby an angular momentum. The angular momentum implies the existence of a magnetic moment vector, μ, and the nuclei can thus interact with a magnetic field.[14,79] The first attempt to measure the nuclear magnetic moment by magnetic resonance was performed by Rabi et al. in 1938.[80] In 1946, Bloch et al.[15] and Purcell et al.[79] independently performed successful experiments detecting magnetic resonance by electromagnetic effects. In the early 1970s, Lauterbur[62,63] described the now used method of how nuclear magnetic resonance could be used for generation of images, and in the beginning of the 1980s rapid development of clinical applications took place.

Basic MRI physics

The most important nucleus used for MRI today is hydrogen (^1H). This nucleus has two possible discrete levels of energy and thereby two possible orientations, explained by quantum mechanics. The spins are equally distributed in these two orientations, unless a static magnetic flux density (magnetic field) B_0 is applied. If so, the spins align with or against B_0 and the magnetic moment vector μ precesses about B_0 with an angular frequency,

$$\omega_0 = \gamma B_0$$

called the Larmor frequency, where $\gamma/2\pi$ equals the gyromagnetic ratio which for ^{1}H is 42.58 MHz/T. The Larmor frequency is equal to the frequency of the electromagnetic radiation associated with possible spin energy transitions.

The summation of all magnetic moment vectors μ within a sample volume can be represented by a macroscopic magnetization vector M. This macroscopic vector is aligned with the external B_0, denoted the z direction. However, when aligned with B_0, the vector M_z can not be detected. In order to detect the magnetization vector, it must be tilted into the xy plane, perpendicular to the z direction. This is performed by a second magnetic field, B_1, applied as a radio frequency (RF) pulse at the Larmor frequency and perpendicular to B_0. This second magnetic field is also called an excitation pulse, since the spin system will be in a higher energy state after application. The angle of rotation away from alignment with the B_0 axis, caused by the excitation pulse, is called the flip angle. During, and directly after excitation, there will be a component of M present in the xy plane perpendicular to z, M_{xy}, oscillating with the Larmor frequency. This M_{xy} may be detected by induction of current in a coil. The observed signal is referred to as the MR signal or free induction decay (FID). If the B_1 applied inverts M_z to $-M_z$, it is called an inversion pulse, i.e. flip angle 180°.

The signal decay can be explained as two independent processes where M_{xy} gradually disappears and M_z gradually recovers. This results from proton interaction where the rate of recovery of M_z is described by the T_1 relaxation time (unit: s) and the disappearance of M_{xy} is described by the T_2 relaxation time (unit: s). The inverse of T_1 and T_2

$$R_1 = 1/T_1$$

$$R_2 = 1/T_2$$

is in turn called the relaxation rate (unit: s^{-1}). The difference in T_1 and T_2 relaxation times in different tissues gives rise to image contrast in T_1-weighted and T_2-weighted images, respectively. The T_1 is the duration of time it takes for 63 % of M_z to recover, and it is dependent on stimulated emission by interaction of fluctuating magnetic fields in the surrounding tissue (spin-lattice interaction). Since T_1 describes the recovery of M_z, it is also called longitudinal recovery or relaxation. The T_2, or transverse relaxation time, is in most cases significantly shorter than M_z recovery, but can be in the order of T_1. The T_2 is the duration of time it takes for M_{xy} to decrease to 37 % of its original value. It is caused by spin-spin interaction and it is dependent on variations in the local magnetic field. The recovery of M_z and decrease of M_{xy} can be described by the following equations.

$$M_z(t) = M_{z0}(1 - e^{-t/T_1})$$
$$M_{xy}(t) = M_{xy0}e^{-t/T_2}$$

MR signal sampling

Magnetic resonance imaging gives the possibility to acquire images in any plane. This is performed by using a magnetic gradient system with three components, that can be combined to select a slice and encode this slice spatially. These components are often referred to as the slice selective, phase encoding, and frequency encoding gradients. Changing the gradient amplitudes over time gives linear variation in the external magnetic field. Thereby spatial encoding is possible.

The MR signal is acquired in the so-called time domain, and through an inverse Fourier transform converted into the frequency domain, which corresponds to the image. The sampling of the MR signal is performed in a coordinate system denoted k-space and is controlled by the chosen pulse sequence, which is a combination of time-varying gradients, timing of excitation, and data acquisition. In order to achieve spatial resolution, signal read-out must be repeated, typically 128 or 256 times. For each echo (signal read-out) the position k_x, k_y is determined by the amplitude and duration of the frequency (k_x) and phase (k_y) encoding gradients. The frequency encoding gradient is on during sampling and one line in k-space is acquired. This is repeated until all lines are filled, each time with a new amplitude of the phase encoding gradient. This way of sampling is denoted 2D cartesian sampling, but sampling may also be performed spirally, in 3D, or by other means. The time between excitation and signal maximum is called echo time (TE), and the time between two successive excitations is called repetition time (TR). However, the denotion of TR differs between pulse sequences and it is therefore of importance to know its exact meaning in each case for understanding of the final image contrast. For image presentation, the magnitude of the MR signal is most often used. However, it is also possible to extract phase information from the acquired signal, and this may be used for velocity measurements or phase sensitive contrast-enhanced imaging.

Triggering

For syncronizing the data acquisition with the cardiac cycle, different methods may be used. Prospective triggering to the R wave of the ECG gives a fixed number of phases. The temporal resolution is approximately 35 ms, depending on the heart rate and number of phases acquired. The natural variation in RR interval and the time required to trigger, however, causes diastolic information to be lost. Retrospective gating with continous acquisition of data solves this problem. Using this method, calculation of phases is performed after the acquisition. If triggering is not possible, real-time imaging may be used, in which the acquisition of an image takes tens of milliseconds, and hence no major cardiac motion has occurred during sampling.
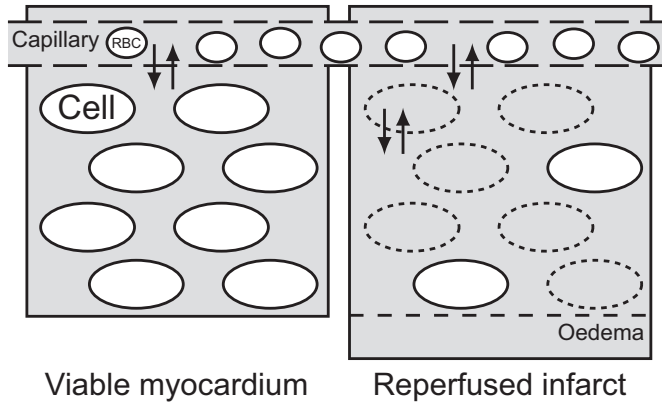
FIGURE 1.1 Schematic drawing of contrast agent distribution, adapted from Arheden et al.[5] The contrast agent distributes passively in the extracellular space, indicated in grey. In reperfused infarction (**right**), the tissue distribution volume is increased compared with viable myocardium. This is mainly due to loss of cellular membrane integrity, and to some extent related to oedema. RBC=red blood cell.

Paramagnetic gadolinium-based contrast agents

In spite of the excellent soft tissue contrast shown by MRI, some situations require increased tissue contrast. The paramagnetic MRI contrast agents predominantly affect the relaxation rates through shortening of T_1,[15,108] and thus it is not the contrast agent that is visualized, but rather the effect exerted on the protons. This effect depends on the number of protons available to affect, the distance to these protons, and the rotational tumbling frequency of the water-particle complex,[61] and may be described by

$$R_{1,\mathrm{post}} = R_{1,\mathrm{pre}} + r_1 C$$

where $R_{1,\mathrm{post}}$ is the relaxation rate after addition of contrast agent, $R_{1,\mathrm{pre}}$ is the original relaxation rate, r_1 is the relaxivity of the contrast agent, and C is the contrast agent concentration. This equation is correspondingly applicable for R_2 calculations. The r_1 *in vitro* is for the agents most often used today approximately 4 $s^{-1}mM^{-1}$ at 20 MHz and 37 °C. The contrast agent concentration in a certain tissue depends on the pharmacokinetics of the contrast agent and tissue architecture. The above equation implies that R_1 is linearly related with contrast agent concentration. *In vivo*, however, this is limited by additional relaxation effects.[30]

The most common paramagnetic agent used today is gadolinium (Gd) which has seven unpaired electrons and thereby high relaxivity.[61] Since Gd is toxic, it is chelated to a ligand, such as DTPA, DOTA, or DTPA-BMA, in order to reduce toxicity.[59] Gd bound to any of the mentioned ligands distributes in the extracellular space[60] and acts mainly on T_1. Since signal intensity in the image is not necessarily linearly related to the relaxation rate, R_1 may instead be quantified by using a Look-Locker[24] sequence. This sequence utilizes a single inversion pulse followed by multiple small flip angle excitation pulses. The longitudinal relaxation time can thereby be determined and R_1 quantified.
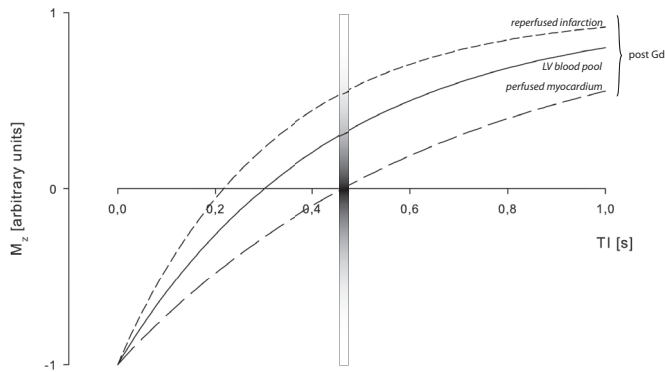

FIGURE 1.2 Longitudinal magnetization recovery curves in the situation when contrast agent has access to the injured myocardium. The reperfused infarct is enhanced in the MR image, due to a larger tissue distribution volume for contrast agent in this region. Optimal TI is chosen as the time when the signal from viable myocardium is nulled. This time point is indicated by the intensity bar, that also indicates the MR image contrast, where black in the MR image corresponds to $M_z=0$, whereas bright regions in the MR image correspond to M_z closer to -1 or 1.

Delayed contrast-enhanced MRI

An inversion recovery (IR) sequence may be used to further increase image contrast between tissues. The sequence consists of an inversion pulse followed by a delay, inversion time (TI), before image acquisition is performed. The TI can be chosen so that signal from a certain tissue is nulled, whereby that tissue becomes black in modulus-based inversion-recovery images. This is used in delayed contrast-enhanced MR imaging (DE-MRI) where an IR gradient-recalled echo

(GRE) sequence is utilized.[96] Since an infarcted region has a much larger tissue distribution volume compared with viable myocardium, due to sarcolemmal rupture, more contrast agent is present in this region and thereby R_1 is increased according to the above equation.[5,33,54,88,105] The increased distribution volume corresponds to the volume of the now necrotic cells (Figure 1.1). It should be noted that the contrast agent distributes passively in the extracellular space and does not accumulate in, or bind to the injured myocardium.[25] By choosing a TI appropriate for nulling the signal from viable perfused myocardium, the infarcted myocardium becomes bright in the image due to the relatively higher contrast agent concentration in this tissue (Figure 1.2). The optimal inversion time depends on parameters such as sequence timing parameters and contrast agent concentration, and thus time after contrast agent administration and elimination rate.

Chapter 2

Aims of the Work

The general aim of this work was to gain knowledge about the pathophysiology of acute myocardial infarction.

The specific aim for each paper was to

    I. compare the perfusion defect size by SPECT with infarct size by DE-MRI,

   II. compare infarct size assessed by serial and clinical routine sampling of biochemical markers CKMB and cTnT with infarct size by DE-MRI,

 III. investigate whether contrast agent used for viability imaging by DE-MRI enters non-perfused myocardium, and whether this region can become hyperintense by delayed contrast-enhanced MRI, also in the absence of contrast agent in this region,

in order to ultimately

 IV. investigate the time course of acute infarct evolution in humans during the first hours of coronary artery occlusion.

Chapter 3

Materials and Methods

The protocols and procedures were approved by the Research Ethics Committee at Lund University, Sweden (Paper I, II, and IV) and the Ethics Committee for Animal Experiments at Uppsala University, Sweden (Paper III).

All patients (Paper I, II, and IV) were recruited at Lund University Hospital and gave their written informed consent to participate in the studies.

3.1   Human studies (Paper I, II, and IV)

Patients presenting with chest pain and ST elevation on their 12-lead ECG, and without earlier evidence of myocardial infarction, were included prospectively between April 2000 and June 2005. They had an occluded coronary artery by angiography and were treated with primary PCI with stenting and GPIIb/IIIa inhibitor, resulting in TIMI grade 3 flow. All patients were transferred to the coronary care unit for conventional therapy, i.e. thrombocyte aggregation inhibitor, ACE inhibitor, beta receptor inhibitor, and a statin, and had an uncomplicated time course between the acute phase and follow-up.

For Paper II and IV, patients with biochemical markers CKMB and cTnT above clinical reference level before treatment were excluded to assure that temporary opening of the occluded coronary artery did not influence infarct size or release of biochemical markers into peripheral blood.[72]

Of the 729 patients approached for inclusion, most patients did not fulfil the inclusion criteria and were excluded, leaving 21 patients for Paper II and 16 patients for Paper IV. For Paper I, 414 patients were approached and 14 patients were included. Reasons for exclusion are listed in Figure 3.1.

The clinical population studied for Paper I was chosen as a non-revascularized group for comparison with revascularized patients.

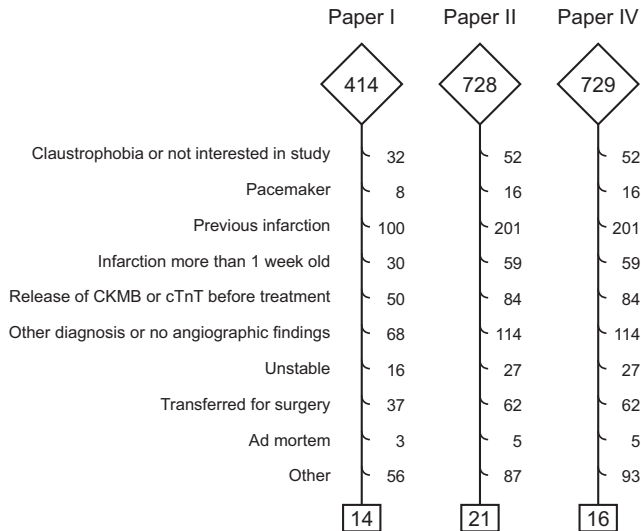|	Paper I	Paper II	Paper IV
	414	728	729
Claustrophobia or not interested in study	32	52	52
Pacemaker	8	16	16
Previous infarction	100	201	201
Infarction more than 1 week old	30	59	59
Release of CKMB or cTnT before treatment	50	84	84
Other diagnosis or no angiographic findings	68	114	114
Unstable	16	27	27
Transferred for surgery	37	62	62
Ad mortem	3	5	5
Other	56	87	93
	14	21	16

FIGURE 3.1 Inclusion-exclusion procedures for the acutely revascularized patient populations for Paper I, II, and IV. For Paper I, patients were included between April 2000 and February 2004, whereas inclusion for Paper II and IV was carried out between April 2000 and June 2005.

For Paper II, serial samples of biochemical markers CKMB and cTnT were acquired prior to revascularization and at 1.5, 3, 6, 12, 18, 24, and 48 hours in 21 patients with an occluded coronary artery. In 17 other patients, clinical routine samples were acquired at arrival, and at 10 and 20 hours for comparison with serial sampling.

Myocardial perfusion SPECT

Patients underwent myocardial perfusion SPECT both in the acute phase for determination of myocardium at risk (Paper IV), and 1 week thereafter for determination of perfusion defect size (Paper I and IV). Perfusion defect size at 1 week was compared with infarct size by DE-MRI (Paper I and IV).

For Paper I, the chronic and clinical study populations underwent myocardial perfusion SPECT on the same day as DE-MRI, and 3.5 days (median) thereafter, respectively.

All patients were administered 500–700 MBq ^{99m}Tc tetrofosmin (Amersham Health, Buckinghamshire, UK), depending on body weight. Within 3 hours, but

not earlier than 30 minutes after isotope administration, myocardial perfusion SPECT was performed according to the standard clinical protocol at rest, using a dual-head gamma camera (ADAC, Milpitas, CA, USA). The patient was placed in supine position and imaged in steps of 5.6 degrees using a 64×64 matrix with a pixel size of 5.02 mm. Image acquisition time was approximately 25 minutes.

Image analysis

Short- and long-axis images covering the left ventricle were reconstructed. This was performed using a commercial application (AutoSpect+InStill™ 6.0, ADAC, Milpitas, CA, USA) with an iterative method (Maximum-Likelihood Expectation-Maximization), using 12 iterations and a Butterworth filter with a cut-off value of 0.6 (of Nyquist)[37] and an order of 5.0.

Analysis of SPECT perfusion defect size is subject to a variety of technical and interpretational issues.[22,31,53,57] We therefore chose to evaluate SPECT data by a validated[38,92] and widely used commercial package (AutoQUANT™ 4.3.1 and a standard database; ADAC, Milpitas, CA, USA), in accordance with clinical practice, rather than to elaborate on the analysis details. However, if the automated method indicated perfusion defect while an experienced reader did not, these regions were excluded from the automated measurement, or vice versa.

Myocardium at risk, perfusion defect size, and left ventricular wall volume were quantified in ml.

MR imaging

Either a 1.5 T system (Magnetom Vision, Siemens, Erlangen, Germany) with a CP body array coil or a 1.5 T system (Philips Intera CV, Philips, Best, the Netherlands) with a cardiac synergy coil was used.

Patients were placed in supine position. Short- and long-axis images covering the left ventricle were acquired. The GRE cine sequence and the segmented IR-GRE sequence were triggered by ECG and images were acquired during breath-holds of approximately 15 seconds. A commercially available gadolinium-based contrast agent (*gadoteric acid*, Gd-DOTA, Guerbet, Gothia Medical AB, Billdal, Sweden) was administered at a dose of 0.2 mmol/kg. Delayed contrast-enhanced MR images were acquired during end diastole at 20 to 40 minutes after contrast agent administration. The TI was adjusted to give null signal from the myocardium.

The volume of the left ventricular wall was measured in the short-axis GRE cine images, and the hyperenhanced volume was measured in the delayed contrast-enhanced IR-GRE images (Table 3.1).

TABLE 3.1

Typical MRI sequence parameters used for the present studies

| | GRE | | IR-GRE | | |
	Siemens[†]	Philips	Siemens[†]	Philips	Look-Locker
TE (ms)	4.8	1.55	3.4	1.21	2.0
TR (ms)	100	3.1	250	3.9	42
FA (°)	20	60	25	15	6
Matrix (×256)	126	160	165	240	154
FOV (mm)	380	400	380	420	300
Slice (mm)	8	8	8	8	10
Gap (mm)	2	-	2	-	-
TI (ms)	-	-	170	255	variable
tr (ms)	50	33	-	-	42
tIR (RR)	-	-	2	1	5

[†] Numaris 3; FA=flip angle; GRE=gradient-recalled echo; IR-GRE=inversion recovery gradient-recalled ehco; RR=R-R interval; TE=echo time; TI=inversion time; TR=repetition time, as indicated in sequence; tr=time resolution; tIR=time between inversion pulses.

Image analysis

All data was analysed using the program ImageJ ver 1.29x (rsb.info.nih.gov/ij). In order to estimate interobserver variability, MR image analysis was performed by two observers, blinded to each others' results as well as information about the patients. For Paper II and IV, the results were also compared with an automated analysis method.[44] The automated method was manually corrected in slices where infarction was seen but missed by the algorithm, or vice versa.

Left ventricular wall volume and hyperenhanced volume were determined in end-diastolic images whereas end-systolic measurements served as an internal control. Endocardial and epicardial borders were manually delineated in each end-diastolic and end-systolic frame in each short-axis stack, covering the left ventricle (Figure 3.2A). Papillary muscles were included as left ventricular wall volume. In the base of the left ventricle where the left atrium was seen, only that portion of the slice which could be identified as left ventricle was included.

Hyperenhanced volume was delineated in the short-axis delayed contrast-enhanced IR-GRE images (Figure 3.2B). The long-axis images were used to verify the distribution of the hyperenhanced region.

Left ventricular wall volume and hyperenhanced volume were calculated as the planimetric measurements of each slice multiplied by slice thickness plus slice gap. Relative hyperenhanced volume was expressed as percentage of the left ventricular
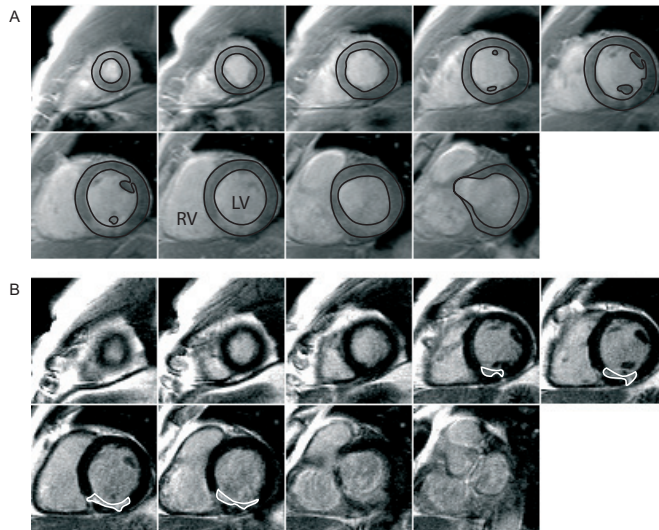
FIGURE 3.2 Short-axis slices from apex to base in a patient with an acute infarct in the inferior wall. The endocardial and epicardial borders are delineated in the cine MR images **(A)**, and the infarct is delineated in the delayed contrast-enhanced MR images **(B)**. LV=left ventricle, RV=right ventricle.

wall volume. For evaluation of the time course of infarct evolution in humans, infarct size by DE-MRI was normalized to myocardium at risk by SPECT (Paper IV).

Biochemical markers (Paper II)

The CKMB and cTnT were determined by standard procedures by the acute clinical chemistry laboratory at Lund University Hospital, using an electrochemiluminescence immunoassay (Hitachi Modular-E, Roche, Mannheim, Germany).

For analysis of peak and cumulative values, patients reaching levels above the maximum value reported by the clinical chemistry laboratory, and patients without all samples assessed, were excluded from that particular analysis.

If CKMB was less than 10 μg/l, and cTnT was less than 0.05 μg/l, they were considered below reference level of infarction. Peak value and cumulative value, calculated as the area under the curve, were used for comparison with infarct size measured by DE-MRI.

Time course of infarct evolution (Paper IV)

Duration of ischaemia was defined as time from onset of chest pain to opening of the occluded coronary artery by PCI. Infarct size was normalized to myocardium at risk for comparison among patients, and for comparing the findings of infarct evolution in humans with several other species from previous animal studies.[6,34,43,55,83–85,94]

3.2 Animal study (Paper III)

Swedish farm pigs of either sex with a weight of 31 ± 5 kg (26–40 kg) were studied. The pigs were sedated and anaesthetized with intramuscular (i.m.) zolazepamtiletamine 6 mg/kg and i.m. xylazine 2.2 mg/kg followed by morphine 20 mg administered through an ear vein. They were tracheotomized and ventilated using a ventilator (Siemens-Elema servo ventilator 900C, Solna, Sweden). The pigs were also fitted with catheters in one of the carotid and one of the femoral arteries, in both ear veins and in one jugular vein. Anaesthesia was maintained by continuously infusing ketamine 20 mg/kg/h and morphine 0.48 mg/kg/h. Pancuronium bromide 6 mg was given for muscle relaxation when necessary.

Myocardial ischaemia was induced by permanent occlusion of the left anterior descending coronary artery. The animals underwent MRI after 200 minutes of occlusion. After MRI, persistent occlusion was verified by angiography and by injection of fluorescein, a marker of perfusion, whereafter the animals were euthanized by administration of potassium chloride. The heart was excised and cut at the same short-axis level as where MR imaging was performed. The injured myocardium was visualized by triphenyltetrazolium chloride (TTC) staining.[32]

MR imaging

Imaging was performed during free breathing at a 1.5 T Gyroscan Intera system (Philips Medical Systems, Best, the Netherlands), using a 20 cm circular receive-only surface coil and triggered by ECG. Data for R_1 measurements was acquired in a short-axis midventricular slice, using a single slice Look-Locker[24] sequence at baseline prior to administration of Gd-DTPA-BMA at a dose of 0.2 mmol/kg, and followed by 13 acquisitions during 1 hour. Each acquisition was collected over 4 minutes and 40 seconds. A non-selective inversion pulse was followed by 70 slice-selective excitation pulses starting at a TI of 14 ms with an increment of 42 ms between excitations, yielding 70 data points on the modulus inversion recovery curve (Table 3.1).

The distance from apex to the short-axis slice was measured in a diastolic long-axis view for later slicing and staining of the myocardium.

Image analysis

Quantitative analysis of the data in the dynamic Look-Locker series was performed using dedicated software by A. Bjørnerud (DimView; now nICE, Nordic-NeuroLab AS, Oslo, Norway). Parametric R_1 maps and corresponding χ^2 error maps[12] (Figure 3.3) were calculated from a non-linear least-squares fit of the Look-Locker data to the equation

$$SI(TI) = \beta|1 - 2e^{-R_1\,TI}| + K$$

where SI is signal intensity, $|\cdot|$ denotes the absolute value, TI is the inversion time, β and K are fitting constants and $R_1 = 1/T_1$ is the model parameter to be determined.[11] Correction was applied for imperfect 180° inversion pulse, partial longitudinal relaxation due to short TR, and alteration of the longitudinal relaxation related to the excitation pulses.
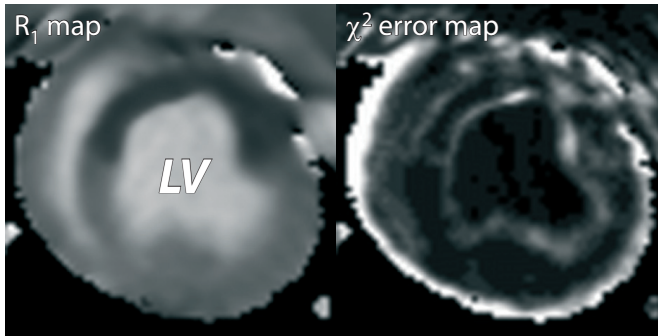
FIGURE 3.3 Parametric R_1 map (**left**) and the corresponding error map (**right**), which reflects the relative error in the curve fit. High signal intensity in the error map indicates regions with poor curve fit due to cardiac motion. These regions were avoided for measurements. LV=left ventricle.

R_1 was measured at each time point in the left ventricular blood pool and in perfused and non-perfused myocardium. The χ^2 error map was used to guide positioning of the region of interest to avoid visual artifacts, edges of myocardium, or pixels that moved between regions during the cardiac cycle. The standard deviation (SD) of R_1 was used as a control to avoid regions with high noise. For each time point after contrast agent adminstration, ΔR_1 was defined as the difference between R_1 at that time point ($R_{1,\text{time}}$) and R_1 before contrast agent administration ($R_{1,\text{baseline}}$), for comparison among regions and among animals.

The intensity of the non-perfused myocardium was visually evaluated in images where the signal from perfused myocardium was nulled, as performed using delayed contrast-enhanced MRI.

3.3   Statistical analyses

SPSS 12.0.1 was used for statistical analyses. Overall, values were expressed as mean $\pm$ SD and $P<0.05$ was considered statistically significant. Bland-Altman plots[13] were used to show differences between measurements (Paper I and IV). Wilcoxon signed-rank test (Paper I) and Mann-Whitney U test (Paper II) were used to test for statistical significance between groups. For the results in Paper III, t distribution was assumed for calculating the 95 % confidence interval, and statistical significance was stated when 95 % confidence intervals did not overlap. Linear regression (Paper II) and logarithmic curve fit to $y(x) = y_0 + a \ln x$ (Paper IV) were performed.

Chapter 4

Results and Comments

4.1 Human studies (Paper I, II, and IV)

SPECT and MRI measurements are comparable (Paper I)

Even though the hypoperfused defect size by SPECT was generally slightly larger than infarct size by DE-MRI, measurements by the two techniques did not differ much for revascularized infarcts (Table 4.1). This is of interest when normalizing infarct size by DE-MRI to myocardium at risk assessed by SPECT, as was performed for determining the impact of duration of ischaemia on infarct size in humans (Paper IV).

TABLE 4.1

Differences between SPECT and MRI measurements in the respective study populations (Paper I)

	Acute	Chronic	Clinical
LVWV (ml)	-23 ± 22	-36 ± 26	0 ± 46
LVWV (%)[†]	-13 ± 11	-18 ± 11	2 ± 24
Defect (ml)	8 ± 8	10 ± 18	26 ± 30
Defect (% LVWV)	6 ± 5	6 ± 11	12 ± 10

LVWV=left ventricular wall volume. Defect=perfusion defect by SPECT, infarct by DE-MRI.
[†] Per cent of MRI LVWV.

Systematic differences between SPECT and MRI may be due to technical issues such as temporal and spatial resolution, but could also be influenced by biological phenomena. While DE-MRI gives the possibility to depict the infarcted

region more directly, SPECT depicts the perfusion defect, i.e. both the infarcted myocardium and a border zone of hypoperfused but viable myocardium.[84]

A better agreement between SPECT and MRI was found for revascularized myocardial infarction (Figure 4.1A,B), compared with non-revascularized infarction (Figure 4.1C). This discrepancy may in part be explained by the difference between perfusion defect and infarction, since the non-revascularized infarcts are more likely to have a larger hypoperfused but viable region (hibernating myocardium[19]) than the revascularized infarcts.

With stunned[18,56] or hibernating myocardium present, the absence of thickening-related count increase may be interpreted as a perfusion defect by SPECT,[74] and thereby lead to an overestimation compared with infarct size by DE-MRI. Furthermore, wall thinning may be detected as perfusion defect by SPECT and this may be part of the explanation for larger perfusion defect sizes measured by SPECT compared to infarct sizes by DE-MRI in the clinical population.[31,100]

The left ventricular wall volume was measured smaller by SPECT than with MRI (Table 4.1). This is most likely an underestimation by SPECT, since previous studies show that MRI correlates well with autopsy findings.[21,65]

Peak biochemical markers can estimate infarct size (Paper II)

For the serial sampling group, an early peak of biochemical markers was found in all patients after revascularization (CKMB: 7.6 ± 3.6 h; cTnT: 8.1 ± 3.4 h), indicating successful revascularization.[49,58,72] The peak values were found at 3, 6, or 12 hours after revascularization, but not at 1.5 hours or after 12 hours. After 48 hours, serum levels of CKMB had returned to below reference value in 12 patients (60 %), whereas serum levels of cTnT remained above reference value in all patients (Figure 4.2).

Peak values correlated better with infarct size by DE-MRI if serial sampling was performed, compared with clinical routine sampling (Figure 4.3). This was especially true for CKMB, that showed no statistically significant correlation to infarct size by DE-MRI, if sampled according to clinical routine. This reflects the importance of correct sample timing for assessment of biochemical peak values. If correct timing is achieved, one may substitute serial sampling with only a few samples for estimation of infarct size (Figure 4.4). This is of relevance in the clinical setting, since serial sampling is both more costly and time consuming than single or few samples.

The limited sensitivity for detecting very small infarcts by DE-MRI was noted in three patients with both CKMB and cTnT above clinical reference level, but nevertheless no infarct by DE-MRI. However, other patients had lower values of biochemical markers than these three patients, and still infarct was measurable by DE-MRI. Therefore, no lower level of biochemical markers for determina-
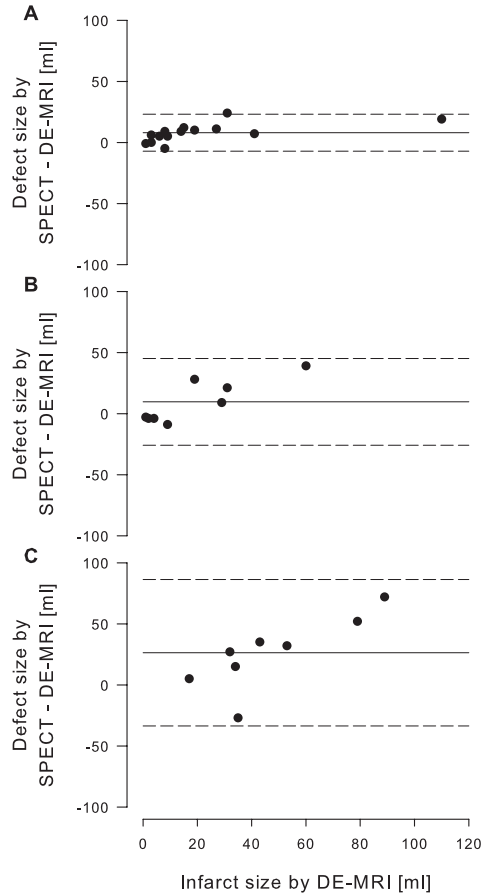
FIGURE 4.1 Agreement between perfusion defect size by SPECT and infarct size by DE-MRI in the acute (**A**), chronic (**B**), and clinical (**C**) populations. Solid lines indicate mean, dashed lines indicates ± 2SD.
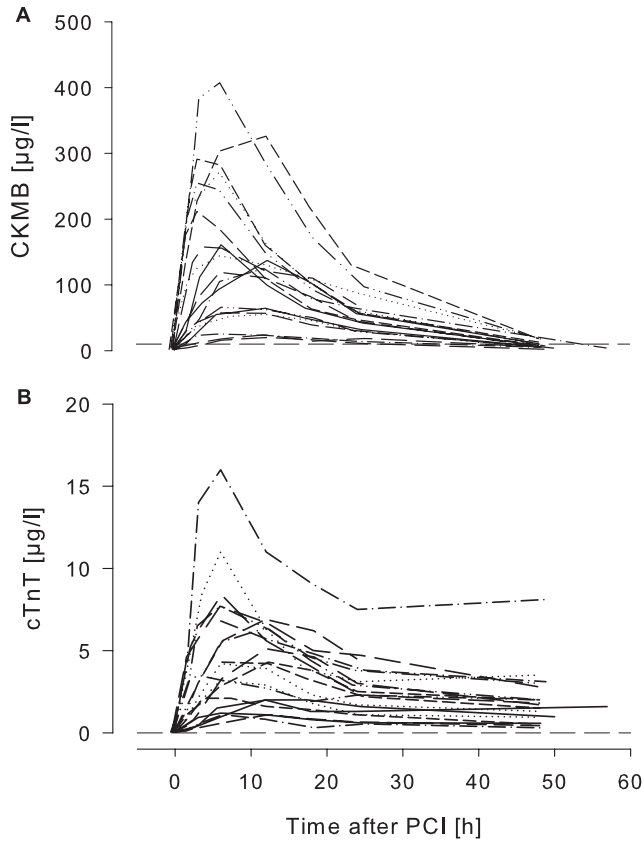
FIGURE 4.2 Serum concentration changes by serial sampling of CKMB **(A)** and cTnT **(B)** from before PCI to 48 hours thereafter. After 48 hours, serum levels of CKMB had returned to below clinical reference value in 12 patients (60 %), whereas serum levels of cTnT remained above clinical reference value in all patients. In one patient, the final sampling was performed at 57 hours. Clinical reference values are indicated by dashed lines.
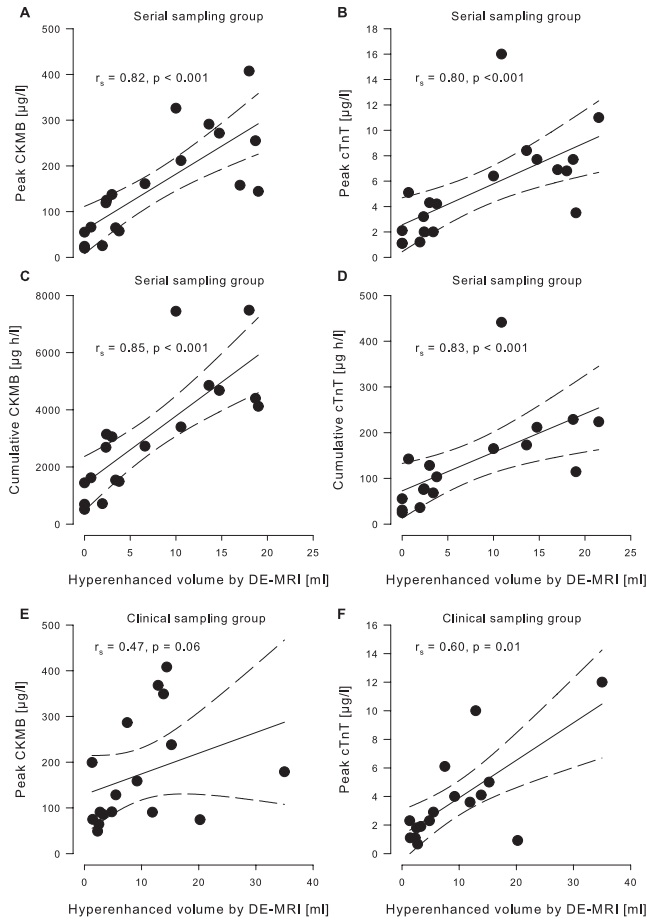
FIGURE 4.3 Biochemical markers compared with infarct size by DE-MRI in the serial and clinical sampling groups. Peak values of both CKMB **(A)** and cTnT **(B)** acquired serially, as well as cumulative values of both CKMB **(C)** and cTnT **(D)**, correlated well with infarct size by DE-MRI. However, peak values acquired by the clinical protocol showed for CKMB **(E)** no statistically significant correlation with infarct size by DE-MRI, and for cTnT **(F)** a somewhat lower correlation compared with serial sampling. Solid lines indicate regression lines. Dashed lines indicate 95 % confidence intervals.

tion of infarction could be established. The sensitivity and specificity for CKMB and cTnT are high, and thereby it has been possible to lower the limit for infarct diagnosis. The clinical implication of low but nevertheless positive values of biochemical markers may, however, need to be further studied.

| Infarct size (ml) | CKMB | | cTnT | |
	peak (µg/l)	cumulative (µg h/l)	peak (µg/l)	cumulative (µg h/l)
2	25	712	1	36
14	291	4850	8	173
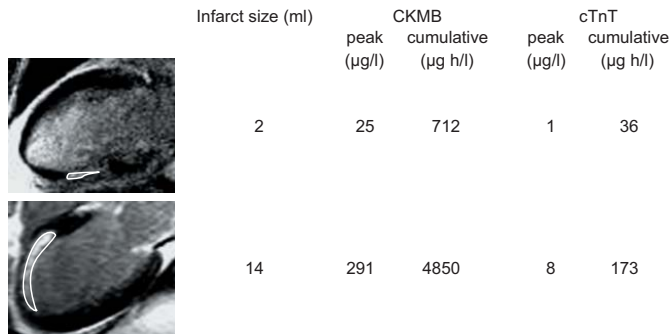
FIGURE 4.4 The relation between biochemical markers by serial sampling and infarct size by DE-MRI visualized for a small infarct **(upper row)**, and a larger infarct **(lower row)**. The infarcted region is outlined in white. LV=left ventricle.

The results from Paper II are not directly applicable in non-revascularized patients, since prolonged leakage of biochemical markers is likely to occur in these patients.[49] Serial sampling may therefore still be needed to estimate infarct size by biochemical markers in non-revascularized patients.

Duration of ischaemia affects infarct size (Paper IV)

Infarct size normalized to left ventricular wall volume could not be shown to depend on duration of ischaemia (Figure 4.5A). This has previously been considered[64] and shown in both dog[83–85] and humans.[42] If infarct size was normalized to myocardium at risk, however, a stronger, but yet statistically unsignificant, correlation was found (Figure 4.5B). Furthermore, three patients in the present study suffered ischaemia for more than 2 hours but nevertheless showed no infarction by DE-MRI. It is not possible to exclude that preconditioning[28,70,71,76] had occurred in these patients, even though they had no history of angina pectoris, or release of biochemical markers before treatment. If these three patients were excluded from the analysis, the correlation between duration of ischaemia and infarct size normalized to left ventricular wall volume increased (Figure 4.5C), and it doubled for infarct size normalized to myocardium at risk, and also became statistically significant (Figure 4.5D).
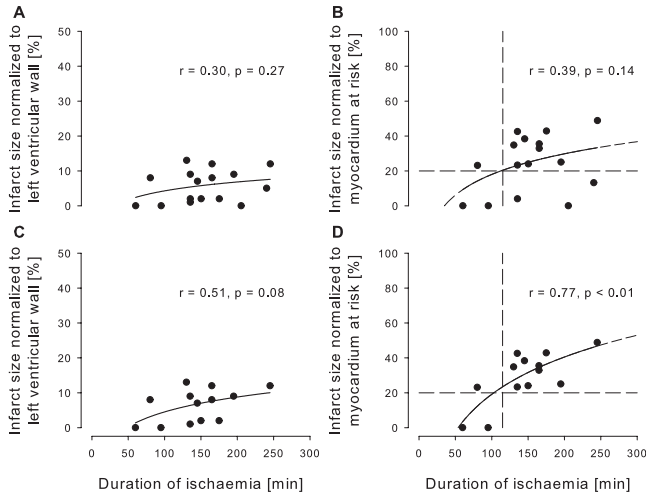
FIGURE 4.5 Relationships between duration of ischaemia and infarct size by DE-MRI normalized to left ventricular volume (A, C) or myocardium at risk (B, D). No statistically significant effect of duration of ischaemia on infarct size normalized to left ventricular wall volume was found **(A)**. A stronger, but yet statistically unsignificant, correlation was found when infarct size was normalized to myocardium at risk. The logarithmic curve fit indicates that approximately 20 % of myocardium at risk was infarcted after approximately 2 hours of occlusion (dashed lines) **(B)**. Three patients had duration of ischaemia longer than 2 hours, but nevertheless no or small infarction by DE-MRI. If these patients were excluded from the analysis, correlation for infarct size normalized to left ventricular wall volume increased **(C)**, and doubled for infarct size normalized to myocardium at risk, and also became statistically significant **(D)**. The curve fit also indicated a faster infarct evolution. Solid lines indicate the logarithmic curve fits within the intervals of the observations, while the extrapolations are shown dashed.

Infarct evolution in humans was found to occur more slowly than in pig and rat, but at a rate similar to that reported for baboon and some canines (Figure 4.6). It should, however, be noted that there is a large variation in infarct evolution, also within species.[34,55,67,83,84]
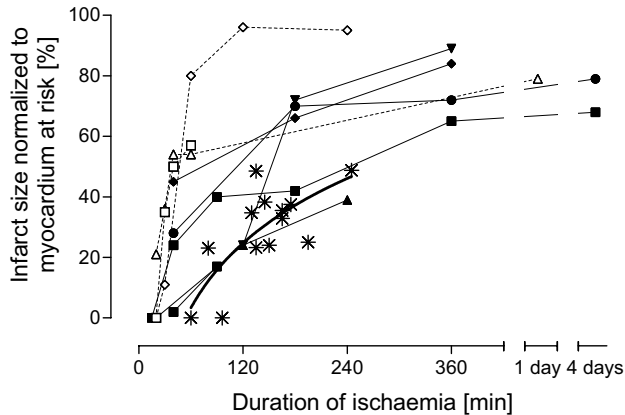

FIGURE 4.6 Infarct size normalized to myocardium at risk with respect to duration of ischaemia in different species. Humans (stars, thick solid line), dog, and baboon (closed symbols, solid lines), were found to have similar time courses of infarct evolution, whereas rat and pig (open symbols, dashed lines) had a more rapid time course of infarct evolution. Note the variation in time courses, also within species. Animal data presented are from several previous studies.[6,34,43,55,83–85,94]

Since the degree of collateral flow is a proven modifier of infarct size,[40,81,89] the difference in time course between species could be explained by lack of collaterals in rat and pig.[67,99] It is generally accepted that collaterals are present in humans, although poorly developed.[7,35] Considering the possibility of a more gradual development of occlusive atherosclerosis in patients compared with experimental animals, it is not unlikely that infarct evolution should occur slower in humans since a higher degree of collateralization could be expected. In the present study, however, only patients with first time myocardial infarct without collaterals visible by angiography, and with biochemical markers below clinical reference level before treatment, were included. Therefore, it is not likely that differences in collateralization is the only explanation to the diverse time courses between species. The diverse time courses may also be explained by disparate protective

mechanisms, and different supply and demand of the ischaemic myocardium in different species. The impact of duration of ischaemia on infarct size in humans is visualized in Figure 4.7.

The time from onset of symptoms to opening of the occluded coronary artery is dependent on information from the patient. There is, however, no reason to believe that any major spontaneous reperfusion occurred between occlusion and PCI, since that would have led to release of biochemical markers.[49]
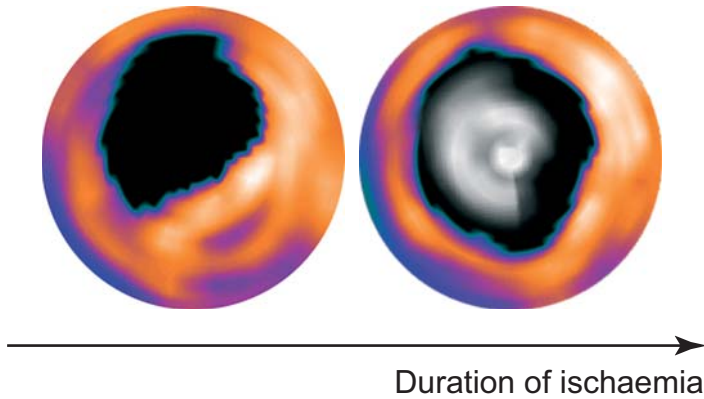

Duration of ischaemia

FIGURE 4.7 Two SPECT polar plots indicating myocardium at risk (black) in the otherwise well perfused myocardium (yellow). Final infarct size from DE-MRI is shown in white, where brightness indicates transmurality. Duration of ischaemia and final infarct size as per cent of myocardium at risk was 95 minutes and 0 % **(left)** and 200 minutes and 40 % **(right)**, respectively.

Finally, even though late revascularization may be of value,[51,77,86] 20–40 % of myocardium at risk was infarcted after 2–3 hours of occlusion and therefore timely revascularization is of great importance to limit infarct size in humans.

Interobserver variability

Overall interobserver variability was for left ventricular wall volume 1 ± 4 ml ($0 \pm 3\%$), and for infarct size 0 ± 1 ml ($1 \pm 3\%$). Overall variability between observer 1 and the automated method[44] (Paper II and IV) was for infarct size -4 ± 6 ml. The automated method was corrected in approximately 5 % of the slices.

4.2 Animal study (Paper III)

MR contrast agent does not enter non-perfused myocardium

Immediately after administration of Gd-DTPA-BMA, a major increase in R_1 was found in blood and perfused myocardium, but not in non-perfused myocardium. During 1 hour thereafter, ΔR_1 in blood and perfused myocardium declined, whereas ΔR_1 in non-perfused myocardium did not change over time. Furthermore, during this hour ΔR_1 was significantly lower in non-perfused myocardium compared with ΔR_1 in both blood and perfused myocardium (Figure 4.8), which indicates absence of contrast agent in non-perfused myocardium. A perfused in-
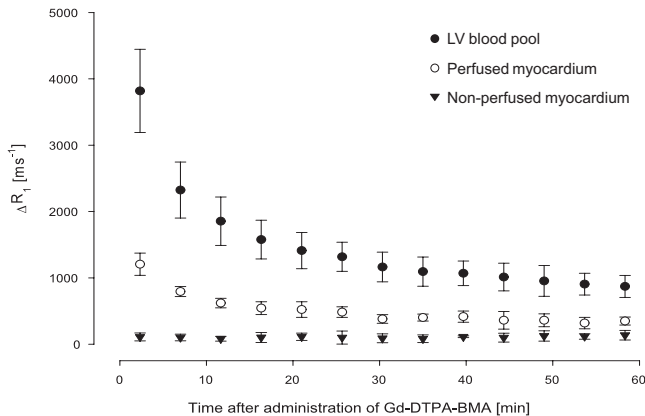
FIGURE 4.8 Changes (compared with baseline) in relaxation rates in blood, perfused myocardium, and non-perfused myocardium, during 1 hour after contrast agent administration. ΔR_1 differed significantly between non-perfused myocardium and both blood and perfused myocardium. Error bars indicate 95 % confidence intervals. LV=left ventricle; $\Delta R_1 = R_{1,time} - R_{1,baseline}$.

farct is hyperintense when nulling the signal from viable perfused myocardium. This is because of larger tissue distribution volume in the infarcted region, compared with blood and viable perfused myocardium.[5,54,91,105]

It has been suggested by some investigators that extracellular Gd-based contrast agents may diffuse into regions of low perfusion.[26,47,52] Others, however, have indicated the importance of flow for delivery of contrast agents into injured myocardium.[20,29,45,66,75,110] The present results show that Gd-DTPA-BMA does

not enter injured non-perfused myocardium (Figure 4.8), and thereby that flow is necessary for delivery of contrast agent. Therefore, in the case of occlusion with no flow, the high intensity seen in the non-perfused myocardium, compared with blood and viable perfused myocardium, is due to absence of contrast agent (Figure 4.8 and Figure 4.9). When nulling the signal from perfused myocardium,
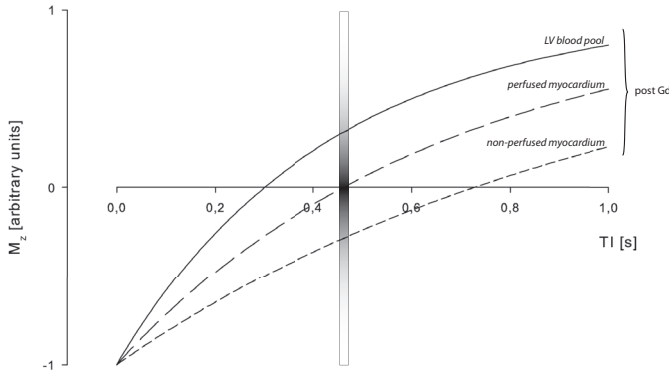

FIGURE 4.9 Longitudinal magnetization recovery curves after administration of an extracellular Gd-based contrast agent, in the situation when contrast agent does not have access to the injured myocardium (non-perfused). The higher signal intensity in non-perfused myocardium is related to modulus reconstruction of the MR image, and is due to absence of contrast agent in this region. The shaded bar indicates intensities in the image (c.f. Figure 4.10). Curves are derived from measured R_1 values 21 minutes after contrast agent administration, but presented as phase-sensitive data for clarity. LV=left ventricle; M_z=magnetic moment in z-direction; TI=inversion time.

as performed for DE-MRI, demarcation of the hyperintense non-perfused myocardium was possible in all animals (Figure 4.10). The high intensity is related to modulus reconstruction of the image data, and may be overcome using phase information.[50] This is however not yet implemented as a standard for viability imaging.

The grey infarcts by DE-MRI that may be seen in some patients can be explained by partial volume effects, but it is important to point out that situations may exist with intermediate levels of contrast agent present in injured myocardium, and this region may therefore be more or less indiscernible from blood or viable perfused myocardium.
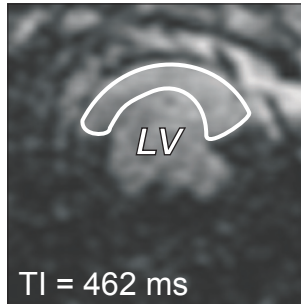
FIGURE 4.10 A short-axis image of the left ventricle acquired 21 minutes after contrast agent administration, using a Look-Locker sequence. The inversion time has been chosen for nulling the signal from perfused myocardium, as performed for viability imaging by DE-MRI. The non-perfused myocardium appears bright, despite lack of contrast agent in this region (outlined in white). LV=left ventricle; RV=right ventricle; TI=inversion time.

Even though a trend toward higher R_1 was found 50–60 minutes after contrast agent administration, this should not be of importance for viability imaging since this most often is performed within 60 minutes and optimally at 20–30 minutes.[54]

One may argue that the beating heart may increase delivery speed, but since approximately 5,000 heart beats did not affect the delivery in a no-flow model, this is not likely to occur. However, in humans with a potentially higher degree of collateralization, increased delivery speed because of movement of the beating heart can not be excluded to occur by these results only. Factors that affect the presence of contrast agent in a certain region, and thereby increased intensity by DE-MRI, are e.g. flow, tissue distribution volume, and time after administration.

The results from Paper III may not be directly applicable to human studies, especially in chronic ischaemia when collateral supply may be further increased. However, the results are relevant for imaging of acute ischaemia and for the basic pathophysiological understanding of inversion-recovery viability imaging.

It was noted that before administration of contrast agent, R_1 in perfused myocardium was higher than in non-perfused myocardium, which in turn was higher than in blood. The small change in R_1 directly after contrast agent administration may be related to contamination by voxels from the blood-pool or perfused myocardium with high R_1. This may need to be investigated using higher spatial and temporal resolution.

Chapter 5

Major Conclusions

The major conclusion of each paper was that:

I. The SPECT perfusion defect size was generally slightly larger than infarct size by DE-MRI, but did not differ much for revascularized infarcts.

II. The peak value of both CKMB or cTnT, assessed at 3, 6, and 12 hours after acute revascularization of an occluded coronary artery, constituted good estimates of cumulative values and correlated well with infarct size by DE-MRI.

III. The extracellular MR contrast agent Gd-DTPA-BMA did not enter non-perfused myocardium within 1 hour after administration during acute coronary occlusion. Despite the absence of contrast agent in this region, the non-perfused myocardium appeared bright when nulling the signal from perfused myocardium using inversion-recovery DE-MRI.

IV. Myocardial infarct size increased as duration of ischaemia increased, to encompass 20–40 % of myocardium at risk after 2–3 hours. This suggests that a major part of myocardium at risk may be salvaged in humans suffering from acute coronary occlusion, if the occlusion is treated within the first hour.

Bibliography

1. Effectiveness of intravenous thrombolytic treatment in acute myocardial infarction. Gruppo Italiano per lo Studio della Streptochinasi nell'Infarto Miocardico (GISSI). *Lancet*, 1(8478):397–402, 1986.

2. Randomised trial of intravenous streptokinase, oral aspirin, both, or neither among 17,187 cases of suspected acute myocardial infarction: ISIS-2. ISIS-2 (Second International Study of Infarct Survival) Collaborative Group. *Lancet*, 2(8607):349–60, 1988.

3. N Al-Saadi, E Nagel, M Gross, A Bornstedt, B Schnackenburg, C Klein, W Klimek, H Oswald, and E Fleck. Noninvasive detection of myocardial ischemia from perfusion reserve based on cardiovascular magnetic resonance. *Circulation*, 101(12): 1379–83, 2000.

4. JS Alpert, K Thygesen, E Antman, and JP Bassand. Myocardial infarction redefined– a consensus document of The Joint European Society of Cardiology/American College of Cardiology Committee for the redefinition of myocardial infarction. *J Am Coll Cardiol*, 36(3):959–69, 2000.

5. H Arheden, M Saeed, CB Higgins, DW Gao, J Bremerich, R Wyttenbach, MW Dae, and MF Wendland. Measuremet of the distribution volume of gadopentetate dimeglumine at echo-planar MR imaging to quantify myocardial infarction: comparison with 99mTc-DTPA autoradiography in rats. *Radiology*, 211(3):698–708, 1999.

6. H Arheden, M Saeed, CB Higgins, DW Gao, PC Ursell, J Bremerich, R Wyttenbach, MW Dae, and MF Wendland. Reperfused rat myocardium subjected to various durations of ischemia: estimation of the distribution volume of contrast material with echo-planar MR imaging. *Radiology*, 215(2):520–8, 2000.

7. G Baroldi, O Mantero, and G Scomazzoni. The collaterals of the coronary arteries in normal and pathologic hearts. *Circ Res*, 4(2):223–9, 1956.

8. SR Bergmann. Clinical applications of myocardial perfusion assessments made with oxygen-15 water and positron emission tomography. *Cardiology*, 88(1):71–9, 1997.

9. DS Berman, H Kiat, and J Maddahi. The new 99mTc myocardial perfusion imaging agents: 99mTc-sestamibi and 99mTc-teboroxime. *Circulation*, 84(3 Suppl):I7–21, 1991.

10. MA Bernstein, KF King, and XJ Zhou. *Handbook of MRI pulse sequences*. Elsevier Academic Press, London, 2004.

11. A Bjornerud, LO Johansson, K Briley-Saebo, and HK Ahlstrom. Assessment of T1 and T2* effects in vivo and ex vivo using iron oxide nanoparticles in steady state–dependence on blood volume and water exchange. *Magn Reson Med*, 47(3):461–71, 2002.

12. A Bjornerud, T Bjerner, LO Johansson, and HK Ahlstrom. Assessment of myocardial blood volume and water exchange: theoretical considerations and in vivo results. *Magn Reson Med*, 49(5):828–37, 2003.

13. JM Bland and DG Altman. Statistical methods for assessing agreement between two methods of clinical measurement. *Lancet*, 1(8476):307–10, 1986.

14. F Bloch. Nuclear induction. *Phys Rev*, 70:460–474, 1946.

15. F Bloch, WW Hansen, and M Packard. Nuclear Induction. *Phys Rev*, 69:127, 1946.

16. E Boersma and ML Simoons. Reperfusion strategies in acute myocardial infarction. *Eur Heart J*, 18(11):1703–11, 1997.

17. R Bracewell and A Riddle. Inversion of fan-beam scans in radioastronomy. *Astrophys J*, 150:427–434, 1967.

18. E Braunwald and RA Kloner. The stunned myocardium: prolonged, postischemic ventricular dysfunction. *Circulation*, 66(6):1146–9, 1982.

19. E Braunwald and JD Rutherford. Reversible ischemic left ventricular dysfunction: evidence for the "hibernating myocardium". *J Am Coll Cardiol*, 8(6):1467–70, 1986.

20. J Bremerich, MF Wendland, H Arheden, R Wyttenbach, DW Gao, JP Huberty, MW Dae, CB Higgins, and M Saeed. Microvascular injury in reperfused infarcted myocardium: noninvasive assessment with contrast-enhanced echoplanar magnetic resonance imaging. *J Am Coll Cardiol*, 32(3):787–93, 1998.

21. GR Caputo, D Tscholakoff, U Sechtem, and CB Higgins. Measurement of canine left ventricular mass by using MR imaging. *AJR Am J Roentgenol*, 148(1):33–8, 1987.

22. L Ceriani, E Verna, L Giovanella, L Bianchi, G Roncari, and GL Tarolo. Assessment of myocardial area at risk by technetium-99m sestamibi during coronary artery occlusion: comparison between three tomographic methods of quantification. *Eur J Nucl Med*, 23(1):31–9, 1996.

23. MJ Davies. The composition of coronary-artery plaques. *N Engl J Med*, 336(18): 1312–4, 1997.

24. Look DC and D Locker. Time saving measurement of NMR and EPR relaxation times. *Rev Sci Instrum*, 41:250–251, 1970.

25. UK Decking, VM Pai, H Wen, and RS Balaban. Does binding of Gd-DTPA to myocardial tissue contribute to late enhancement in a model of acute myocardial infarction? *Magn Reson Med*, 49(1):168–71, 2003.

26. P Dendale, PR Franken, M Meusel, R van der Geest, and A de Roos. Distinction between open and occluded infarct-related arteries using contrast-enhanced magnetic resonance imaging. *Am J Cardiol*, 80(3):334–6, 1997.

27. EG DePuey, EV Garcia, and DS Berman. *Cardiac SPECT imaging*. Lippincott Williams & Wilkins, Philadelphia, second edition, 2001.

28. E Deutsch, M Berger, WG Kussmaul, Jr. Hirshfeld, JW, HC Herrmann, and WK Laskey. Adaptation to ischemia during percutaneous transluminal coronary angioplasty. Clinical, hemodynamic, and metabolic features. *Circulation*, 82(6):2044–51, 1990.

29. PW Doherty, MJ Lipton, WH Berninger, CG Skioldebrand, E Carlsson, and RW Redington. Detection and quantitation of myocardial infarction in vivo using transmission computed tomography. *Circulation*, 63(3):597–606, 1981.

30. KM Donahue, RM Weisskoff, and D Burstein. Water diffusion and exchange as they influence contrast enhancement. *J Magn Reson Imaging*, 7(1):102–10, 1997.

31. RL Eisner and RE Patterson. The challenge of quantifying defect size and severity: reality versus algorithm. *J Nucl Cardiol*, 6(3):362–71, 1999.

32. MC Fishbein, S Meerbaum, J Rit, U Lando, K Kanmatsuse, JC Mercier, E Corday, and W Ganz. Early phase acute myocardial infarct size quantification: validation of the triphenyl tetrazolium chloride tissue enzyme staining technique. *Am Heart J*, 101(5):593–600, 1981.

33. SJ Flacke, SE Fischer, and CH Lorenz. Measurement of the gadopentetate dimeglumine partition coefficient in human myocardium in vivo: normal distribution and elevation in acute and chronic infarction. *Radiology*, 218(3):703–10, 2001.

34. H Fujiwara, M Matsuda, Y Fujiwara, M Ishida, A Kawamura, G Takemura, M Kida, T Uegaito, M Tanaka, K Horike, and et al. Infarct size and the protection of ischemic myocardium in pig, dog and human. *Jpn Circ J*, 53(9):1092–7, 1989.

35. WF Fulton. Arterial Anastomoses in the Coronary Circulation. I. Anatomical Features in Normal and Diseased Hearts Demonstrated by Stereoarteriography. *Scott Med J*, 143:420–34, 1963.

36. V Fuster, B Stein, JA Ambrose, L Badimon, JJ Badimon, and JH Chesebro. Atherosclerotic plaque rupture and thrombosis. Evolving concepts. *Circulation*, 82 (3 Suppl):II47–59, 1990.

37. G Germano. Technical aspects of myocardial SPECT imaging. *J Nucl Med*, 42(10): 1499–507, 2001.

38. G Germano, PB Kavanagh, P Waechter, J Areeda, S Van Kriekinge, T Sharir, HC Lewin, and DS Berman. A new algorithm for the quantitation of myocardial perfusion SPECT. I: technical principles and reproducibility. *J Nucl Med*, 41(4): 712–9, 2000.

39. RJ Gibbons, TD Miller, and TF Christian. Infarct size measured by single photon emission computed tomographic imaging with (99m)Tc-sestamibi: A measure of the efficacy of therapy in acute myocardial infarction. *Circulation*, 101(1):101–8, 2000.

40. MG Gottwik, S Puschmann, B Wusten, C Nienaber, KD Muller, M Hofmann, and W Schaper. Myocardial protection by collateral vessels during experimental coronary ligation: a prospective study in a canine two-infarction model. *Basic Res Cardiol*, 79 (3):337–43, 1984.

41. EM Haacke, RW Brown, MR Thompson, and R Venkatesan. *Magnetic Resonance Imaging: Physical Principles and Sequence Design*. John Wiley & Sons, 1999.

42. J Haase, R Bayar, M Hackenbroch, H Storger, M Hofmann, CE Schwarz, H Reinemer, F Schwarz, J Ruef, and T Sommer. Relationship between size of myocardial infarctions assessed by delayed contrast-enhanced MRI after primary PCI, biochemical markers, and time to intervention. *J Interv Cardiol*, 17(6):367–73, 2004.

43. SL Hale and RA Kloner. Effect of early coronary artery reperfusion on infarct development in a model of low collateral flow. *Cardiovasc Res*, 21(9):668–73, 1987.

44. E Heiberg, H Engblom, J Engvall, E Hedstrom, M Ugander, and H Arheden. Semiautomatic quantification of myocardial infarction from delayed contrast enhanced magnetic resonance imaging. *In press.*, 2005.

45. CB Higgins, PL Hagen, JD Newell, WS Schmidt, and FH Haigler. Contrast enhancement of myocardial infarction: dependence on necrosis and residual blood flow and the relationship to distribution of scintigraphic imaging agents. *Circulation*, 65 (4):739–46, 1982.

46. BF Hutton and A Osiecki. Correction of partial volume effects in myocardial SPECT. *J Nucl Cardiol*, 5(4):402–13, 1998.

47. RM Judd, CH Lugo-Olivieri, M Arai, T Kondo, P Croisille, JA Lima, V Mohan, LC Becker, and EA Zerhouni. Physiological basis of myocardial contrast enhancement in fast magnetic resonance images of 2-day-old reperfused canine infarcts. *Circulation*, 92(7):1902–10, 1995.

48. HT Karsner and JE Dwyer. Studies in infarction. IV. Experimental bland infarction of the myocardium, myocardial regeneration and cicatrization. *J Med Research*, 34: 21, 1916.

49. HA Katus, A Remppis, T Scheffold, KW Diederich, and W Kuebler. Intracellular compartmentation of cardiac troponin T and its release kinetics in patients with reperfused and nonreperfused myocardial infarction. *Am J Cardiol*, 67(16):1360–7, 1991.

50. P Kellman, AE Arai, ER McVeigh, and AH Aletras. Phase-sensitive inversion recovery for detecting myocardial infarction using gadolinium-delayed hyperenhancement. *Magn Reson Med*, 47(2):372–83, 2002.

51. CB Kim and E Braunwald. Potential benefits of late reperfusion of infarcted myocardium. The open artery hypothesis. *Circulation*, 88(5 Pt 1):2426–36, 1993.

52. RJ Kim, EL Chen, JA Lima, and RM Judd. Myocardial Gd-DTPA kinetics determine MRI contrast enhancement and reflect the extent and severity of myocardial injury after acute reperfused infarction. *Circulation*, 94(12):3318–26, 1996.

53. MA King, DT Long, and AB Brill. SPECT volume quantitation: influence of spatial resolution, source size and shape, and voxel size. *Med Phys*, 18(5):1016–24, 1991.

54. C Klein, SG Nekolla, T Balbach, B Schnackenburg, E Nagel, E Fleck, and M Schwaiger. The influence of myocardial blood flow and volume of distribution on late Gd-DTPA kinetics in ischemic heart failure. *J Magn Reson Imaging*, 20(4): 588, 2004.

55. RA Kloner, SG Ellis, R Lange, and E Braunwald. Studies of experimental coronary artery reperfusion. Effects on infarct size, myocardial function, biochemistry, ultrastructure and microvascular damage. *Circulation*, 68(2 Pt 2):I8–15, 1983.

56. RA Kloner, RB Arimie, GL Kay, D Cannom, R Matthews, A Bhandari, T Shook, C Pollick, and S Burstein. Evidence for stunned myocardium in humans: a 2001 update. *Coron Artery Dis*, 12(5):349–56, 2001.

57. A Kojima, M Matsumoto, M Takahashi, Y Hirota, and H Yoshida. Effect of spatial resolution on SPECT quantification values. *J Nucl Med*, 30(4):508–14, 1989.

58. JA Kragten, WT Hermens, and MP van Dieijen-Visser. Cumulative troponin T release after acute myocardial infarction. Influence of reperfusion. *Eur J Clin Chem Clin Biochem*, 35(6):459–67, 1997.

59. H Kroll, S Korman, E Siegel, HE Hart, B Rosoff, H Spencer, and D Laszlo. Excretion of yttrium and lanthanum chelates of cyclohexane 1,2-trans diamine tetraacetic acid and diethylenetriamine pentaacetic acid in man. *Nature*, 180(4592):919–20, 1957.

60. P Kruhoffer. Inulin as an indicator for the extracellular space. *Acta Physiol Scand*, 11:16–36, 1945.

61. R Lauffer. Paramagnetic metal complexes as water proton relaxation agents for NMR imaging: theory and design. *Chem Rev*, 87:901–927, 1987.

62. PC Lauterbur. Magnetic resonance zeugmatography. *Pure Appl Chem*, 50:149–157, 1974.

63. PC Lauterbur. Image formation by induced local interactions: examples employing nuclear magnetic resonance. *Nature*, 242(5394):190–1, 1973.

64. JE Lowe, KA Reimer, and RB Jennings. Experimental infarct size as a function of the amount of myocardium at risk. *Am J Pathol*, 90(2):363–79, 1978.

65. GK Lund, MF Wendland, A Shimakawa, H Arheden, F Stahlberg, CB Higgins, and M Saeed. Coronary sinus flow measurement by means of velocity-encoded cine MR imaging: validation by using flow probes in dogs. *Radiology*, 217(2):487–93, 2000.

66. T Masui, M Saeed, MF Wendland, and CB Higgins. Occlusive and reperfused myocardial infarcts: MR imaging differentiation with nonionic Gd-DTPA-BMA. *Radiology*, 181(1):77–83, 1991.

67. MP Maxwell, DJ Hearse, and DM Yellon. Species variation in the coronary collateral circulation during regional myocardial ischaemia: a critical determinant of the rate of evolution and extent of myocardial infarction. *Cardiovasc Res*, 21(10):737–46, 1987.

68. TD Miller, TF Christian, MR Hopfenspirger, DO Hodge, BJ Gersh, and RJ Gibbons. Infarct size after acute myocardial infarction measured by quantitative tomographic 99mTc sestamibi imaging predicts subsequent mortality. *Circulation*, 92(3):334–41, 1995.

69. TR Miller and JW Wallis. Clinically important characteristics of maximum-likelihood reconstruction. *J Nucl Med*, 33(9):1678–84, 1992.

70. CE Murry, RB Jennings, and KA Reimer. Preconditioning with ischemia: a delay of lethal cell injury in ischemic myocardium. *Circulation*, 74(5):1124–36, 1986.

71. Y Nakagawa, H Ito, M Kitakaze, H Kusuoka, M Hori, T Kuzuya, Y Higashino, K Fujii, and T Minamino. Effect of angina pectoris on myocardial protection in patients with reperfused anterior wall myocardial infarction: retrospective clinical evidence of "preconditioning". *J Am Coll Cardiol*, 25(5):1076–83, 1995.

72. U Naslund, S Haggmark, G Johansson, K Pennert, S Reiz, and SL Marklund. Effects of reperfusion and superoxide dismutase on myocardial infarct size in a closed chest pig model. *Cardiovasc Res*, 26(2):170–8, 1992.

73. FJ Neumann, M Gawaz, T Dickfeld, A Wehinger, H Walter, R Blasini, and A Schomig. Antiplatelet effect of ticlopidine after coronary stenting. *J Am Coll Cardiol*, 29(7):1515–9, 1997.

74. K Nichols, EG DePuey, MI Friedman, and A Rozanski. Do patient data ever exceed the partial volume limit in gated SPECT studies? *J Nucl Cardiol*, 5(5):484–90, 1998.

75. S Nilsson, G Wikstrom, A Ericsson, M Wikstrom, A Waldenstrom, and A Hemmingsson. MR imaging of gadolinium-DTPA-BMA-enhanced reperfused and non-reperfused porcine myocardial infarction. *Acta Radiol*, 36(6):633–40, 1995.

76. F Ottani, M Galvani, D Ferrini, F Sorbello, P Limonetti, D Pantoli, and F Rusticali. Prodromal angina limits infarct size. A role for ischemic preconditioning. *Circulation*, 91(2):291–7, 1995.

77. MA Pfeffer and E Braunwald. Ventricular remodeling after myocardial infarction. Experimental observations and clinical implications. *Circulation*, 81(4):1161–72, 1990.

78. GM Pohost, RA O'Rourke, DS Berman, and PM Shah. *Imaging in cardiovascular disease*. Lippincott Williams & Wilkins, Philadelphia, 1st edition, 2000.

79. EM Purcell, HC Torrey, and RV Pound. Resonance absorption by nuclear magnetic moments in a solid. *Phys Rev*, 69:37–38, 1946.

80. II Rabi, JR Zacharias, S Millman, and P Kusch. New method of measuring nuclear magnetic moment (letter). *Phys Rev*, 53:318, 1938.

81. KB Ramanathan, JL Wilson, LA Ingram, and DM Mirvis. Effects of immature recruitable collaterals on myocardial blood flow and infarct size after acute coronary occlusion. *J Lab Clin Med*, 125(1):66–71, 1995.

82. SI Rapaport and LV Rao. The tissue factor pathway: how it has become a "prima ballerina". *Thromb Haemost*, 74(1):7–17, 1995.

83. KA Reimer and RB Jennings. The "wavefront phenomenon" of myocardial ischemic cell death. II. Transmural progression of necrosis within the framework of ischemic bed size (myocardium at risk) and collateral flow. *Lab Invest*, 40(6):633–44, 1979.

84. KA Reimer, JE Lowe, MM Rasmussen, and RB Jennings. The wavefront phenomenon of ischemic cell death. 1. Myocardial infarct size vs duration of coronary occlusion in dogs. *Circulation*, 56(5):786–94, 1977.

85. KA Reimer, RS Vander Heide, and VJ Richard. Reperfusion in acute myocardial infarction: effect of timing and modulating factors in experimental models. *Am J Cardiol*, 72(19):13G–21G, 1993.

86. V Richard, CE Murry, and KA Reimer. Healing of myocardial infarcts in dogs. Effects of late reperfusion. *Circulation*, 92(7):1891–901, 1995.

87. PA Rinck. *Magnetic Resonance in Medicine*. Blackwell Publishers, Oxford, 4th edition, 2001.

88. M Saeed, MF Wendland, T Masui, and CB Higgins. Reperfused myocardial infarctions on T1- and susceptibility-enhanced MRI: evidence for loss of compartmentalization of contrast media. *Magn Reson Med*, 31(1):31–9, 1994.

89. J Schaper and W Schaper. Time course of myocardial necrosis. *Cardiovasc Drugs Ther*, 2(1):17–25, 1988.

90. UJ Schoepf, CR Becker, BM Ohnesorge, and EK Yucel. CT of coronary artery disease. *Radiology*, 232(1):18–37, 2004.

91. J Schwitter, M Saeed, MF Wendland, N Derugin, E Canet, RC Brasch, and CB Higgins. Influence of severity of myocardial injury on distribution of macromolecules: extravascular versus intravascular gadolinium-based magnetic resonance contrast agents. *J Am Coll Cardiol*, 30(4):1086–94, 1997.

92. T Sharir, G Germano, PB Waechter, PB Kavanagh, JS Areeda, J Gerlach, X Kang, HC Lewin, and DS Berman. A new algorithm for the quantitation of myocardial perfusion SPECT. II: validation and diagnostic yield. *J Nucl Med*, 41(4):720–7, 2000.

93. WK Shen, BK Khandheria, WD Edwards, JK Oh, Jr. Miller, FA, JM Naessens, and AJ Tajik. Value and limitations of two-dimensional echocardiography in predicting myocardial infarct size. *Am J Cardiol*, 68(11):1143–9, 1991.

94. YT Shen, JT Fallon, M Iwase, and SF Vatner. Innate protection of baboon myocardium: effects of coronary artery occlusion and reperfusion. *Am J Physiol*, 270(5 Pt 2):H1812–8, 1996.

95. LA Shepp and BF Logan. The Fourier reconstruction of a head section. *IEEE Trans Nucl Sci*, NS-21:21–43, 1974.

96. OP Simonetti, RJ Kim, DS Fieno, HB Hillenbrand, E Wu, JM Bundy, JP Finn, and RM Judd. An improved MR imaging technique for the visualization of myocardial infarction. *Radiology*, 218(1):215–23, 2001.

97. AJ Sinusas, KA Trautman, JD Bergin, DD Watson, M Ruiz, WH Smith, and GA Beller. Quantification of area at risk during coronary occlusion and degree of myocardial salvage after reperfusion with technetium-99m methoxyisobutyl isonitrile. *Circulation*, 82(4):1424–37, 1990.

98. AJ Sinusas, Q Shi, MT Saltzberg, P Vitols, D Jain, FJ Wackers, and BL Zaret. Technetium-99m-tetrofosmin to assess myocardial blood flow: experimental validation in an intact canine model of ischemia. *J Nucl Med*, 35(4):664–71, 1994.

99. PO Sjoquist, G Duker, and O Almgren. Distribution of the collateral blood flow at the lateral border of the ischemic myocardium after acute coronary occlusion in the pig and the dog. *Basic Res Cardiol*, 79(2):164–75, 1984.

100. WH Smith, RJ Kastner, DA Calnon, D Segalla, GA Beller, and DD Watson. Quantitative gated single photon emission computed tomography imaging: a counts-based method for display and measurement of regional and global ventricular systolic function. *J Nucl Cardiol*, 4(6):451–63, 1997.

101. JA Sorenson and ME Phelps. *Physics in nuclear medicine*. WB Saunders, Philadelphia, 1987.

102. BS Sridhara, S Braat, P Rigo, R Itti, P Cload, and A Lahiri. Comparison of myocardial perfusion imaging with technetium-99m tetrofosmin versus thallium-201 in coronary artery disease. *Am J Cardiol*, 72(14):1015–9, 1993.

103. HW Strauss, K Harrison, JK Langan, E Lebowitz, and B Pitt. Thallium-201 for myocardial imaging. Relation of thallium-201 to regional myocardial perfusion. *Circulation*, 51(4):641–5, 1975.

104. N Takahashi, CP Reinhardt, R Marcel, and JA Leppo. Myocardial uptake of 99mTc-tetrofosmin, sestamibi, and 201Tl in a model of acute coronary reperfusion. *Circulation*, 94(10):2605–13, 1996.

105. CY Tong, FS Prato, G Wisenberg, TY Lee, E Carroll, D Sandler, J Wills, and D Drost. Measurement of the extraction efficiency and distribution volume for Gd-DTPA in normal and diseased canine myocardium. *Magn Reson Med*, 30(3): 337–46, 1993.

106. BM Tsui, GT Gullberg, ER Edgerton, JG Ballard, JR Perry, WH McCartney, and J Berg. Correction of nonuniform attenuation in cardiac SPECT imaging. *J Nucl Med*, 30(4):497–507, 1989.

107. T Varetto, D Cantalupi, A Altieri, and C Orlandi. Emergency room technetium-99m sestamibi imaging to rule out acute myocardial ischemic events in patients with nondiagnostic electrocardiograms. *J Am Coll Cardiol*, 22(7):1804–8, 1993.

108. HJ Weinmann, RC Brasch, WR Press, and GE Wesbey. Characteristics of gadolinium-DTPA complex: a potential NMR contrast agent. *AJR Am J Roentgenol*, 142(3):619–24, 1984.

109. A Younes, JA Songadele, J Maublant, E Platts, R Pickett, and A Veyre. Mechanism of uptake of technetium-tetrofosmin. II: Uptake into isolated adult rat heart mitochondria. *J Nucl Cardiol*, 2(4):327–33, 1995.

110. KK Yu, M Saeed, MF Wendland, MW Dae, S Velasquez-Rocha, N Derugin, and CB Higgins. Comparison of T1-enhancing and magnetic susceptibility magnetic resonance contrast agents for demarcation of the jeopardy area in experimental myocardial infarction. *Invest Radiol*, 28(11):1015–23, 1993.

111. DP Zipes, P Libby, RO Bonow, and E Braunwald. *Braunwald's Heart Disease: A Textbook of Cardiovascular Medicine*. W.B. Saunders Company, Philadelphia, 7th edition, 2004.

Acknowledgments

and continous discussions on that subject and others. **Inga-Lill Enochsson**, nurse, for flexibility and always finding time reservable for acute cardiac MR examinations.

Nurses and physicians at the cardiac catheterization laboratory for calling when a patient arrived, thereby making inclusion possible. Especially I would like to thank nurses **Jonas Möller**, **Mathilda Odklev**, **Ronnie Svensson**, and **David Zughaft**.

Physician **Attila Fregyesi** for his enthusiasm, calling the evening of New Year's Eve, and other nights. **Nurses at the coronary care unit** for support with acquiring biochemical markers. Physicians **Karin Åström-Olsson**, **Hans Öhlin**, and **Fredrik Frogner** for help with acute SPECT and MR examinations. Other **physicians** that with short notice have managed to help with these examinations when the three above could not.

Professor **Håkan Ahlström**, **Tomas Bjerner**, PhD, **Rolf Eriksson**, PhD, and **Lars Johansson**, for invaluable discussions during the experiments and ever since, their positive attitude, and never giving up. Also **technicians Agneta Ronéus**, **Karin Fagerbrink**, and **Anne Abrahamsson** for help with animal preparation.

Axel & Chans for the refreshing walks and lively discussions about life in general. **My family**: Margareta, Lennart, Karin, and Carl, for their love, patience, support, for introducing me to the wonderful world of natural science, and for reminding me that the most important object of life is not magnetic resonance imaging, even though I did not always listen. **Minna Carlsson**, for her love and support in every aspect, and understanding my way of prioritization.

Erik Hedström
Lund 2005